Influence of desorption conditions before gas separation studies in nanocomposite MFI – alumina membranes

A. Alshebani[1], M. Pera-Titus[1], K.L. Yeung[2], S. Miachon[1,*] and J.-A. Dalmon[1]

[1] *Institut de Recherches sur la Catalyse et l'Environnement de Lyon (IRCELYON), UMR 5256 CNRS - Université Claude Bernard Lyon 1, 2, av. A. Einstein, 69626 Villeurbanne cedex, France*

[2] *Department of Chemical Engineering, The Hong Kong University of Science and Technology (HKUST), Clear Water Bay, Kowloon, Hong Kong, China*

Abstract

The gas permeation and separation performance of polycrystalline MFI-type zeolite membranes is strongly dependent on the number and type of intercrystalline pores in its structure. Herein we show that the role of such domains is affected by how a membrane is pre-treated before use to remove adsorbed species (e.g. moisture and organics). This 'pre-treatment' step appears to be crucial not only to obtain reliable permeation data, but also to improve the membrane separation performance in practical applications. We illustrate this idea by using a collection of tubular nanocomposite MFI-alumina membranes showing different quality for the separation of n-butane/H_2 mixtures and submitted to different pre-treatment protocols. The influence of each protocol on the final separation performance of the membranes depends on their quality, namely on the density of intercrystalline defects or non-zeolite pores in their structure. Moreover the quality of the support affects the final membrane performance.

Keywords: MFI membrane, pre-treatment, gas separation, n-butane, hydrogen, support quality

1. Introduction

The separation performance of polycrystalline zeolite membranes is directly related to the amount of intercrystalline defects they may include. These defects or non-zeolite pores usually consist of mesopores and grain boundaries larger than the zeolite micropores, but can also include pinholes and cracks. The formation of cracks is especially critical in film-like configurations. In this case, the thermal expansion mismatch between the support and the zeolite layer can lead to crack formation during template removal by calcination and further cooling, or to grain boundary opening when operated at elevated temperatures [1-5]. This translates in practice into a low reproducibility, which makes the scale-up of film-like zeolite membranes difficult.

In some recent studies, we have shown the potentials of nanocomposite MFI-type zeolite membranes to overcome the above stated thermal limitations [6]. In this concept, the active phase is not made of a film on top of a porous support, but rather embedded into the support pores. Compared to film-like structures, the individual membrane defects, if any, cannot exceed the size of the support pore. Moreover, the active phase is protected by the hard matrix of the support. This limits the formation of long-range stresses and provides higher resistance to thermal shocks. Finally, due to the intimate composite structure at the nanoscale, the thermal behaviour of nanocomposite membranes is different from their film-like counterparts [4,7]. This translates into an improved gas separation performance at high temperatures (>400 K).

Several techniques have been used for defect characterization in polycrystalline zeolite membranes, including microscopy (e.g. SEM, HRTEM and AFM) [8,9], Hg porosimetry [10] and permporometry [11]. Inspired in this latter technique, we have shown in the past [12] that dynamic desorption of a gas adsorbed beforehand (e.g., water or n-butane) under pressure difference of a non-adsorbing gas (e.g., hydrogen) provides valuable information on the defective structure of a membrane.

Single-gas permeance measurements constitute the simplest method for a rapid assessment of the presence of defects in zeolite membranes [13-15]. However, these measurements do not always allow direct a discrimination of intercrystalline domains. The most straightforward and reliable way to characterise large pores is from gas separation. Three different kinds of separations can be used, relying in each case on differences in [1,2]: (1) molecular size (molecular sieving), (2) surface diffusion rate, and (3) adsorption strength. The separation of butane/H_2 at low temperature is often used for quality testing as adsorbing/non-adsorbing mixture of gases of different molecular weights [16-19]. In the presence of non-zeolitic crossing pores, H_2 will permeate, even if all zeolite pores are occupied by n-butane molecules. Therefore, the low temperature permeate composition can be used as a sensitive indicator of membrane quality. As a matter of fact, any mesoporous defect in the membrane would locally inverse the selectivity (turning to Knudsen mechanism), and reduce the separation factor. Other tests such as molecular sieving-based separations (e.g., N_2/SF_6) or diffusion-based separations (e.g. n-butane/i-butane) [4] might not be so discriminative, considering that Knudsen-

* Corresponding author. Tel.: +33(0)472445384, Fax: +33(0)472445399, E-mail: sylvain.miachon@ircelyon.univ-lyon1.fr

type defects can either show some separative efficiency (N_2/SF_6), or be neutral (n-butane/i-butane).

The low temperature n-butane/H_2 separation is so sensitive that different laboratories have reported different separation factors on the very same material. This suggests a role of adsorbed species in grain boundaries, either blocking [20] or promoting [12] the permeation of the non-adsorbing species (H_2 in this case). Looking more

Table 1.
Pre-treatment methods prior to gas separation experiments in MFI-type zeolite membranes

Pre-treatment			Butane separation	References
Method	T_{max} [K] / time [h]	Conditions		
(a) *In situ* heating	420 / 2	-	n-C_4H_{10}/i-C_4H_{10}	[21]
	673 / 4	-	n-C_4H_{10}/H_2 H_2/i-C_4H_{10} n-C_4H_{10}/i-C_4H_{10}	[22]
	673 / 4	-	n-C_4H_{10}/i-C_4H_{10}	[23]
	753 / 4-8	-	N_2/n-C_4H_{10}	[24] [a]
	553 / 8	-	n-C_4H_{10}/CH_4 n-C_4H_{10}/i-C_4H_{10}	[25] [b]
(b) *In situ* heating under inert gas flow	673 / 6	N_2 flow (20 NmL·min^{-1})	n-C_4H_{10}/H_2	[6] [c]
	673 / 6	N_2 flow (20 NmL·min^{-1})	n- C_4H_{10}/H_2	[13] [c]
	623 / overnight	He flow (100 NmL·min^{-1})	n-C_4H_{10}/H_2 H_2/i-C_4H_{10} n-C_4H_{10}/i-C_4H_{10}	[26]
	573 / 4	Air flow	n-C_4H_{10}/i-C_4H_{10}	[27]
	753 / 8	He flow (50 NmL·min^{-1})	n-C_4H_{10}/i-C_4H_{10}	[28]
	573 / overnight	He flow	n-C_4H_{10}/i-C_4H_{10}	[29]
	543-673 / 2	N_2 or He flow	n-C_4H_{10}/i-C_4H_{10}	[30]
	500 / 16	He flow	n-C_4H_{10}/i-C_4H_{10}	[31] [a]
	473 / -	He flow (100 NmL·min^{-1})	n-C_4H_{10}/H_2 n-C_4H_{10}/i-C_4H_{10}	[32]
	623 / overnight	He flow (100 NmL·min^{-1})	n-C_4H_{10}/H_2 H_2/i-C_4H_{10} n-C_4H_{10}/i-C_4H_{10}	[33]
	473 / -	He flow (100 NmL·min^{-1})	n-C_4H_{10}/i-C_4H_{10}	[34] [a]
	453 / -	He flow	n-C_4H_{10}/i-C_4H_{10}	[35] [b]
	373 / 12	Air flow	n-C_4H_{10}/i-C_4H_{10}	[36] [b]
	373 / 8	He flow (30 NmL·min^{-1})	H_2/i-C_4H_{10} n-C_4H_{10}/i-C_4H_{10}	[37] [d]
(c) *In situ* heating under vacuum	458 / -	Vacuum	n-C_4H_{10}/i-C_4H_{10}	[38]
	433 / overnight	Vacuum	n-C_4H_{10}/i-C_4H_{10}	[39]
	423 / 16	Vacuum (10^{-3} mbar)	n-C_4H_{10}/i-C_4H_{10}	[40]
	393 / 16	Vacuum (10^{-4} mbar)	CH_4/i-C_4H_{10} H_2/i-C_4H_{10} n-C_4H_{10}/i-C_4H_{10}	[16] [b]
(d) Storage	373 / -	Storage in oven	H_2/i-C_4H_{10}	[41]
	-	Storage at room T under vacuum	n-C_4H_{10}/i-C_4H_{10}	[42]

[a] Only ideal selectivities are reported
[b] Synthesis without template
[c] Nanocomposite membrane
[d] Treatment with an O_3/O_2 mixture (50 ppm) at 473 K for 30 min was also used instead of calcination

carefully into this problem, we present here some evidence of the influence of the desorption step applied to MFI membranes synthesised in our laboratory on their further gas separation performance. Indeed, this 'pre-treatment' procedure, if any, varies quite a lot in the literature. A comprehensive list of reported protocols for membrane pre-treatment before gas permeance and separation measurements together with some heating conditions is provided in Table 1. In general terms, these pre-treatment protocols can be classified in four main groups: (a) *in situ* calcination in air, (b) heating in the permeation under an inert gas flow, (c) heating under vacuum, and (d) simply storage at room temperature in an oven or at ambient temperature under vacuum. As can be seen, most pre-treatment protocols involve heating the membrane under a He or N_2 stream for a given time. However, only few authors have subjected the permeation module to evacuation using vacuum pumping upon heating.

This paper is intended to study the influence of the pre-treatment protocol (cf. Table 1) on the pure gas permeance and separation factors of MFI-type zeolite membranes. Moreover, we will explore how this influence depends on membrane quality.

Another part of this paper is devoted to study the influence of support quality on the final composite membrane performance, both on the single gas permeance and the gas mixture separation.

2. Experimental

2.1. Membrane supports

The membranes were prepared on porous asymmetric 15-cm long tubular supports with 7 mm i.d. and 10 mm o.d. provided by Pall Exekia (Membralox T1-70). These supports consisted of three α-alumina layers (see Fig. 1) with average pore size and thickness decreasing from the outer to the inner side of the tube. Both ends of the supports were enamelled (1 cm at each side) to define a permeation length of 13 cm and an active surface of 0.28 cm^2 and to tighten carbon o-rings during gas transport measurements.

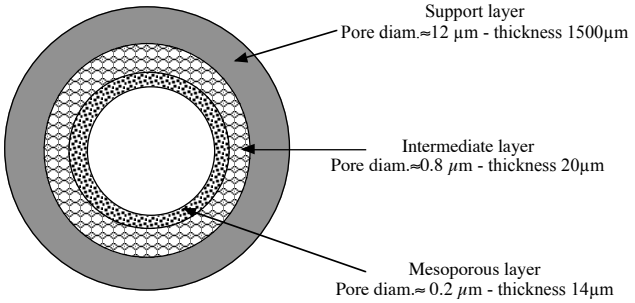

Fig. 1. Schematic cross-section of the membrane showing the three-layered structure

2.2. Porous support bubble flow testing

Prior to synthesis, the porous structure of the supports was characterized by a method based on gas–liquid displacement. In this test, the membranes were mounted in dead-end configuration using flat gaskets pressed onto the enamelled tube-ending cross-section, and then immersed in an ethanol bath for at least 24 h to ensure that all the pores were completely filled by the solvent.

The bubble test was initiated by introducing dry N_2 into the open side of the tubes in dead-end mode, keeping them immersed in ethanol, and measuring the N_2 flow rate. The N_2 pressure was then increased by 5-min steps to liberate ethanol from smaller pores, leading to an increase of N_2 permeance. The pressure at which the first bubble was observed, characterized by the appearance of N_2 permeance (see Fig. 2), allowed the determination of the largest through-pore of the support according to Laplace law (Eq. 1)

$$\Delta P = \frac{4\gamma}{d}\cos(\theta) \qquad (1)$$

where d is the largest pore size, γ is the surface tension of the solvent (23 $mN.m^{-1}$ for ethanol at room temperature), θ is the contact angle (0° for a perfect wetting liquid, the case of ethanol on γ-alumina), and ΔP is the first bubble relative pressure.

A further increase of the permeating gas flow with the applied pressure allowed a relative comparison of tubes of similar structure, with regards to the importance of subsequent smaller defects in the support top layer. In this way, the N_2 flux at 303 kPa was taken as an indication of support quality as mentioned in a previous paper [6]. Let us underline that this analysis is much more severe than what is needed for the strict commercial applications of this type of tubes.

After the tests, the supports were rinsed in distilled water for 30 minutes and dried in an oven overnight (14-16 h) at 120°C. The supports were then cooled down to room temperature. Only supports showing a 3 bar flux <1 $mol{\cdot}m^{-2}{\cdot}s^{-1}$ were used, which was the case for most of them

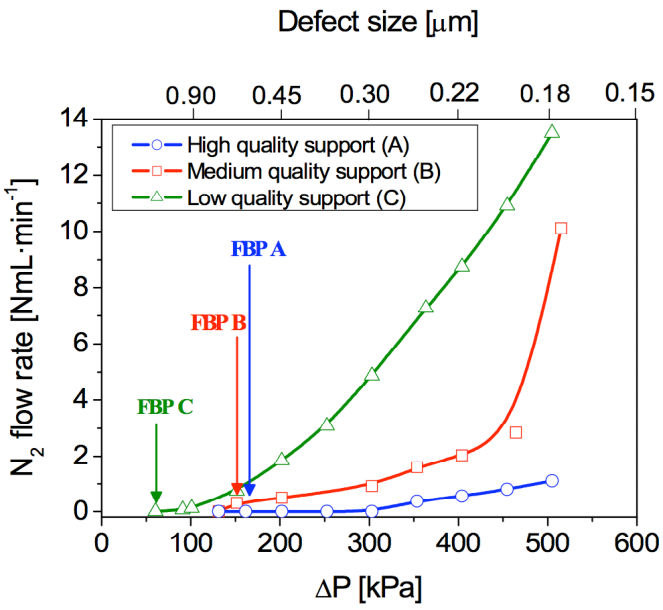

Fig. 2. Bubble test of porous supports (FBP, First Bubble Point). Defect size was estimated using Young-Laplace equation, assuming capillary pores perfectly wetted (contact angle 0°), and using an ethanol surface tension value of 24 $mN.m^{-1}$.

2.3. Hydrothermal synthesis

The nanocomposite MFI-alumina membranes were prepared by *in situ* templated hydrothermal synthesis. A clear solution was obtained by dissolving the silica precursor (Aerosil 380, Degussa) in 1 M tetrapropylammonium hydroxide (TPAOH, Aldrich) to the final molar composition 1.0 SiO_2 : 0.35-0.5 TPAOH : 27.8 H_2O. MFI zeolite was grown at 170ºC for 89 h in the α-alumina support porosity by the pore-plugging technique. More details dealing with nanocomposite MFI-alumina membrane synthesis can be found elsewhere [6].

After the synthesis, the autoclave was cooled down to room temperature, the synthesized membranes were removed, washed with deionized water until a neutral pH was reached, and dried overnight at room temperature and subsequently at 120°C for 12 hours. A N_2 permeation test was then performed to assess for the presence of large defects or cracks at this stage. The dried membranes were then calcined at 500°C for 4 h under air stream with a ramp of 1°C·min^{-1} for template removal following the guidelines of our previous study [6].

2.4. Permeation module

Prior to gas permeance measurements, the membranes were set in a tubular stainless steel module and each ends sealed using graphite seals, as in previous publications [4,7,12]. At this stage, the membranes were subjected to different pre-treatments to remove adsorbed species (see section 2.7 for more details).

2.5. H_2 gas permeation test

After preheating the membrane, single H_2 permeation experiments were performed at room temperature in dead-end mode. Pure H_2 (Air Liquide, 99.99%) was fed to the retentate side of the membrane at 200 kPa, while the permeate side was kept at atmospheric pressure. The H_2 permeance, Π_{H2}, was measured using a DryCal piston volumetric flowmeter, connected to the permeate stream of the membrane. The experimental error of permeance was found to be always lower than 2%.

2.6. *n*-butane / H_2 separation

The set-up used to carry out *n*-butane/H_2 mixture separations is schematically depicted in Fig. 3. The separation tests were performed in a Wicke-Kallenbach permeation cell. The pressure at the feed side was kept at 125 kPa, while the pressure drop between the feed and permeate sides was kept at 0.4 kPa. The mixture was fed to the inner side of the membrane using N_2 as carrier gas. The flow rate of each gas was measured using mass flow controllers (Brooks 5850 TR) and was kept at 55 NmL·min^{-1} for N_2 and 11 NmL·min^{-1} for both n-butane and H_2. N_2 was also used as sweep gas at the permeate side (52 NmL·min^{-1}) in counter-current flow.

The composition at the retentate and permeate sides of the membrane was analyzed by a HP 5890/series II GC equipped with a Porapak Q column and a TCD detector. The separation factor of n-butane over H_2, $Sf_{C4H10/H2}$, was calculated as the permeate-to-feed composition ratio of n-butane, divided by the same ratio for H_2, as in previous studies [6,12]. The separation factor was measured at steady state and room temperature. In all the separations, mass balances were performed with an accuracy better than 5%. Moreover, although the accuracy of the Sf measurement was found to be a function of membrane quality, the data obtained was in all cases statistically significant. It is noteworthy that, in the case of high quality membranes, slight variations of H_2 concentrations can

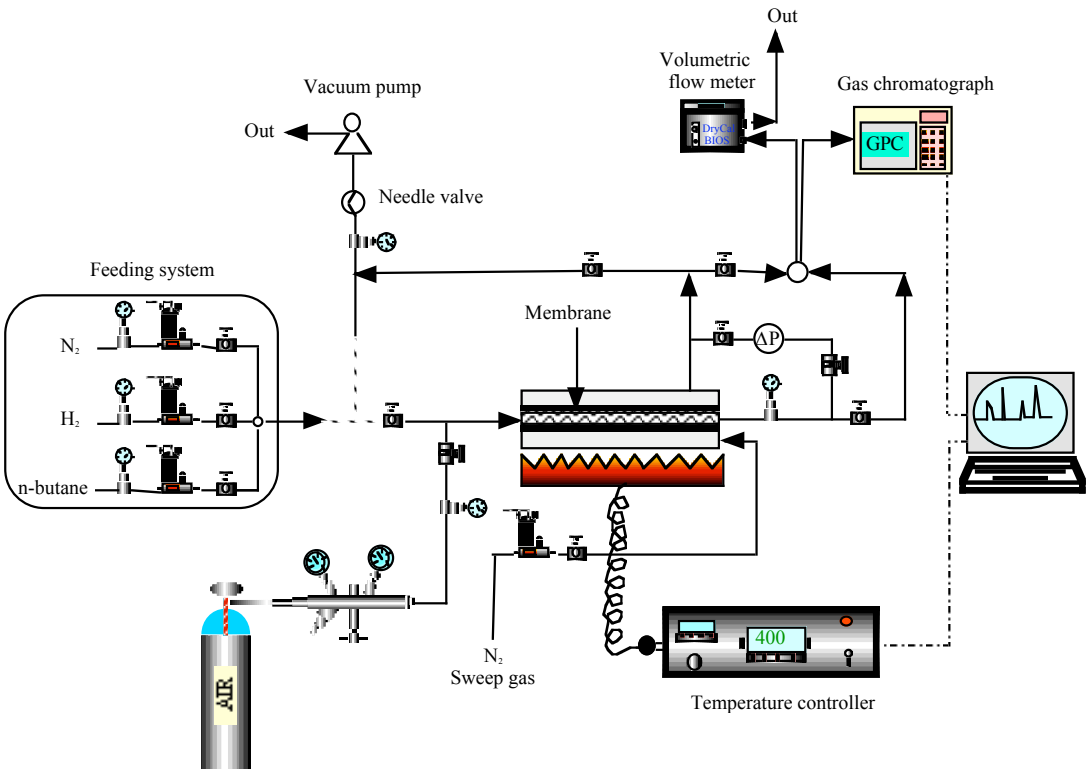

Fig. 3 Experimental set-up forH_2/ n-butane separations

translate into high changes in terms of separation factors, since they pemeate n-butane faster than H_2. This is why the determination of separation factors for high quality membrane usually suffers from lower accuracy when compared to membranes displaying lower quality.

The set of measurements including hydrogen permeance and n-butane/H_2 separation will be denoted as 'performance test' or simply P.T. in the rest of the paper.

2.7. Pre-treatment protocols

Under the guidance of the list of pre-treatment methods in Table 1, four different pre-treatment protocols were tested here. They were compared using single-gas H_2 permeance and n-butane/H_2 selectivity data. These cleaning protocols (i.e. desorption procedures) are schematically depicted in Figs. 4a-d.

2.7.1. Protocol I: Vacuum + 200ºC (Fig. 4a)

The gas in both the retentate and permeate sides of the membrane module was first evacuated at room temperature using a vacuum pump (MVP 035-2, Pfeiffer Vacuum Technology, Germany) for 30 min. The module was then heated to 200°C with a ramp of 1ºC·min^{-1} (3 h) keeping a pressure below 1 mbar for 15 h. The module was then cooled down to room temperature and it was isolated from the vacuum pump. At this point, a N_2 stream (50 NmL·min^{-1}) was sent to both sides of the membrane for 15-30 min, before proceeding to the P.T.

2.7.2. Protocol II: Vacuum + 400ºC (Fig. 4b)

This protocol is similar to protocol I, but here the membrane is heated to 400ºC for 6 h using the same temperature ramp.

2.7.3. Protocol III: N_2 (1 bar) + 400ºC (Fig. 4c)

The membrane module was heated to 400ºC with a heating ramp of 1ºC·min^{-1}, left at this temperature for 6 h under dry N_2 flow at each side of the membrane (20 NmL·min^{-1}) with no transmembrane pressure, and cooled down to room temperature. This protocol was considered as a reference for membrane testing, as used previously [6].

2.7.4. Protocol IV: air (1 bar) + 200ºC (Fig. 4d)

This protocol is similar to protocol III, but this time, the membrane was heated to 200ºC and subjected to a transmembrane pressure of air. Air was used for further calcination, in order to remove any adsorbed hydrocarbons from zeolite pores. The feed pressure was kept at 200 kPa, while the permeate pressure was kept at atmospheric pressure and no sweep gas was used. Further on, the P.T. was carried out.

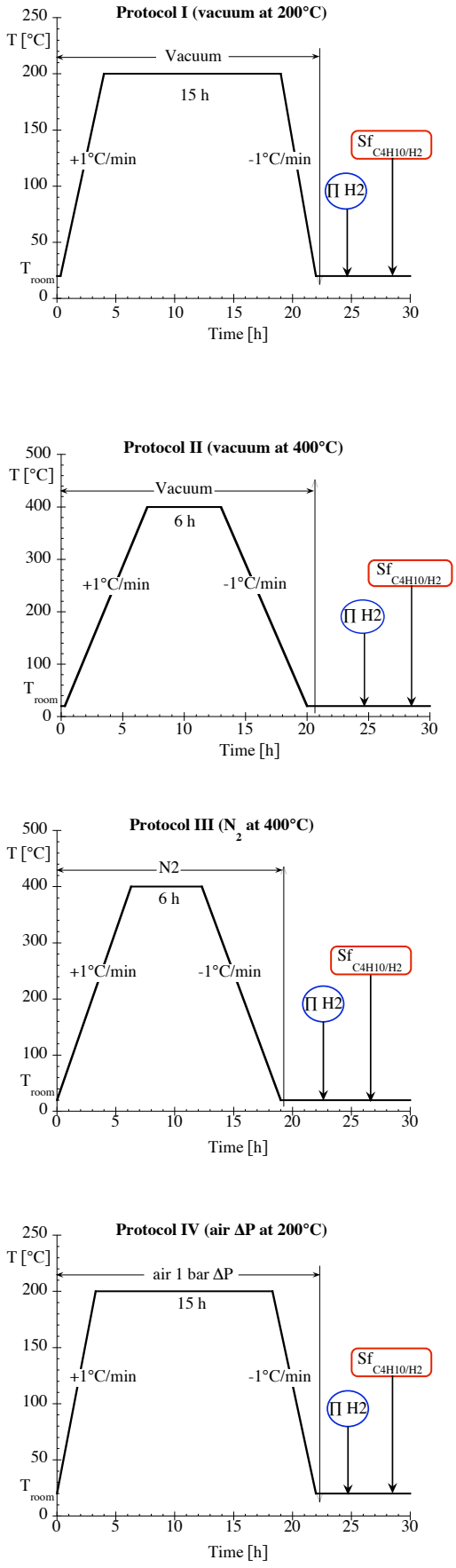

Fig. 4. Heating curves used in protocols I, II, III, and IV. Nomenclature: 'ΠH_2', H_2 permeance; '$Sf_{C4H10/H2}$', separation factor.

2.8. Test succession

The P.T. was carried out on different quality membranes stored in dry air at room temperature, first without pre-treatment before the measurements, and subsequently after successive pre-treatment steps. P.T. was performed after protocol I (vacuum at 200°C) and then after protocol II (vacuum at 400°C). At this stage, the membrane was submitted to air atmosphere before applying protocol III (nitrogen at 400°C) and running the P.T. Then protocol IV (air ΔP at 200°C) was applied before P.T.

The membrane was then submitted to air atmosphere again, before applying protocol IV (air ΔP at 200°C) and P.T. measurement, and protocol III (nitrogen at 400°C) and P.T.

This whole succession is illustrated in the results section (see Fig. 5). Please note that between each cleaning step, the membrane was necessarily saturated by n-butane due to $Sf_{C4H10/H2}$ test. This succession allows for a valid comparison of the desorption efficiency of each protocol. As a matter of fact, when the membranes were not re-submitted to air, prior to desorption protocol II, it was because this protocol applied stronger conditions than that applied immediately before. Indeed, after protocol I, the membrane permeance was not as high as expected (as from the primary characterisation shown in Table 2), thus the decision to apply a stronger desorption conditions.

It should be stressed that for each experiment including a desorption step and a P.T., great care was taken that steady state was reached before measurements. Typical experiments involving both steps would necessitate at least two days. As the whole set of test succession was carried out on the three types of membranes, and some individual measurements were executed at least twice, the results presented in Fig. 5 account for more than 25 tests.

3. Results

3.1. Membrane quality

Table 2 lists the main characteristics of three nanocomposite MFI-type zeolite membranes synthesized in this work on supports of different quality, as observed from pressure of first bubble and N_2 flux at 3 bar. As can be seen, the lower the membrane quality (i.e. the Sf value), the higher the room temperature pure H_2 permeance.

Table 2.
Bare support characterisation by gas-liquid displacement (first bubble pressure and nitrogen flow rate at 300 kPa overpressure), 2nd and 3rd columns. Single-gas H_2 permeance [Π_{H2}, $\mu mol \cdot m^{-2} \cdot s^{-1} \cdot Pa^{-1}$] and n-butane/$H_2$ separation factors ($Sf_{C4H10/H2}$) of the nanocomposite MFI-alumina zeolite membranes synthesized in this study, 4th and 5th columns.

	Support before synthesis		MFI membranes	
Support quality	First bubble ΔP [kPa]	N_2 flow rate at ΔP=300 kPa [$ml \cdot min^{-1}$]	Π_{H2}* [$\mu mol \cdot m^{-2} \cdot s^{-1} \cdot Pa^{-1}$]	$Sf_{C4H10/H2}$*
High (A)	131	0.25	0.26	104
Medium (B)	131	0.9	0.31	28
Low (C)	61	4.9	0.72	3

* Measurements carried out after pre-treatment using protocol III.

3.2. Influence of pre-treatment on gas permeation and separation performance

Fig. 5 summarizes the influence of the four kinds of pre-treatment protocols on the pure H_2 permeation and n-butane/H_2 separation performance for the three membranes listed in Table 2. In all cases, in absence of pre-treatment, both the H_2 permeance and the n-butane/H_2 separation factors are very low. After pre-treatment using protocol I (vacuum at 200°C), the value of both parameters reaches approximately the values shown in Table 2. Protocol II (vacuum at 400°C), applied after butane adsorption during the measurement of n-butane/H_2 separation factors, seems to slightly increase them, except for the lowest quality membrane (C).

After re-submitting the membrane to open atmosphere and subjecting it to new pre-treatment now using protocol III (N_2 flow at 400°C), all the membranes tend to recover their previous pure H_2 permeance and n-butane/H_2 separation factor values, except for the best quality membrane (A), which shows a reduction of about 10%. Further application of protocol IV (air ΔP at 200°C) does not appear to affect the values of both parameters to a great extent.

To further assess for the efficiency of protocol IV in desorbing adsorbed species, it was again applied after re-submitting the membrane to open atmosphere. At this point, both single-gas H_2 permeance and n-butane/H_2 separation factor values were much lower than the former ones. This reduction is larger for the lowest quality membranes. Final recovery of the former values was obtained after another application of protocol III.

4. Discussion

4.1. Influence of support quality on membrane separation performance

As was suggested in former work [6], membrane defects may be ascribed to support defects (i.e. pores larger than the nominal 0.2 μm) that may not be plugged by zeolite during synthesis. The support quality can be inferred from bubble flow. Zeolite membrane quality, in this work, was assessed using n-butane/hydrogen separation at room temperature.

Let us suppose that the hydrogen flux through the membranes during this separation essentially takes place through these unplugged support defects, as estimated from bubble flow. This hydrogen flux is inversely proportional to the n-butane/hydrogen separation factor, as the n-butane concentration in the permeate for all the membranes is similar. Therefore, the bubble flow and Sf should be related, that is, membranes with higher bubble flows should show lower Sfs. This can be visualized when considering Table 2 data, where the product of Sf by the nitrogen flow rate a 300 kPa overpressure is close for the three membranes (20 ± 6 $NmL \cdot min^{-1}$). This result sustains the idea that support quality influences to a great extent the final zeolite membrane quality for separation.

4.2. *Importance of support quality on membrane pure gas permeance*

The three membranes tested here show a relatively large array of pure hydrogen permeance (see Table 2). This could be attributed to differences either in thickness or defect density in the nanocomposite MFI – alumina membranes.

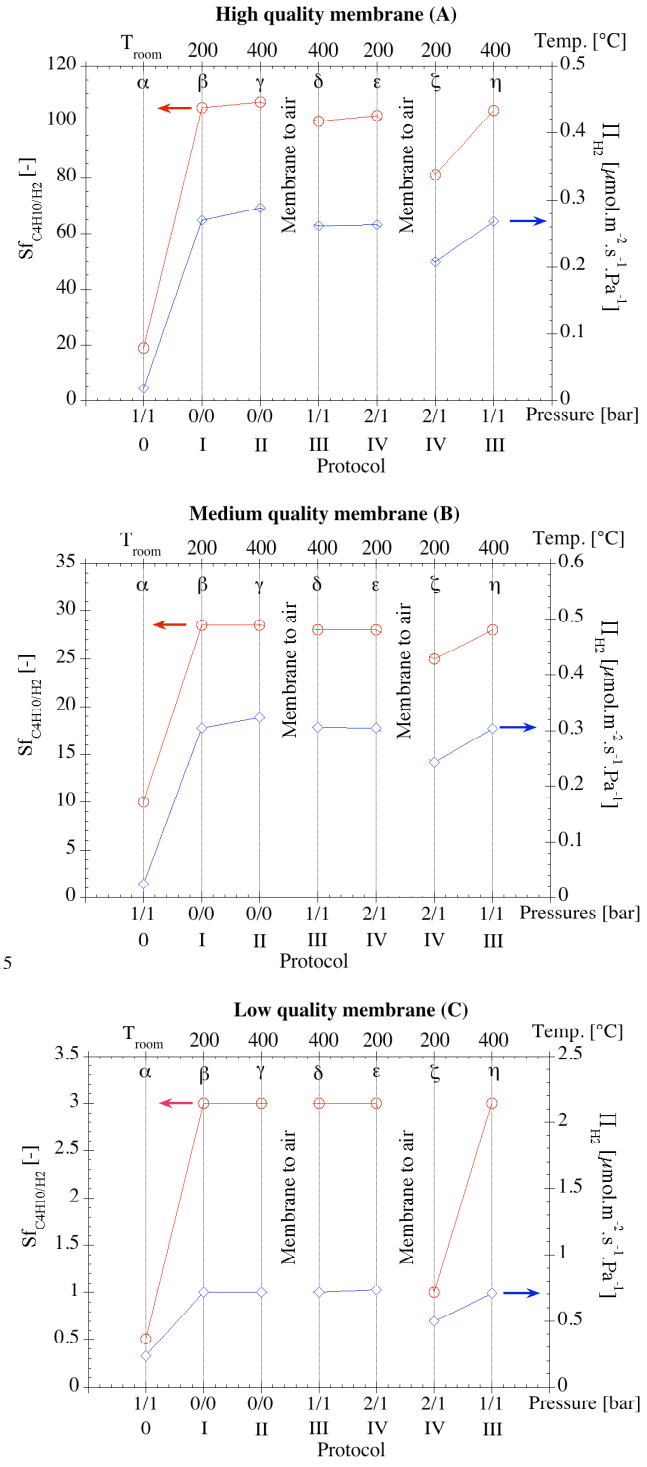

Fig. 5. n-butane/H_2 separation factors and H_2 permeance (P.T.) as a function of pre-treatment for high-quality (A), medium-quality (B), and low-quality nanocomposite MFI-alumina membranes. The lower abscissa axis shows the pre-treatment desorption protocol applied before P.T. in roman numbers and the retentate / permeate pressures applied. The upper abscissa axis shows the maximum temperature applied during desorption.

As mentioned previously, support defects are evidenced during bubble flow test. However, their contribution to the mass transfer for the tested membranes is questionable. Indeed, the pure gas permeance contribution of the support defects can be estimated from Table 2 bubble flow rate data. Even in the case of a low-quality support (membrane C), this contribution is only ~0.004 $\mu mol \cdot m^{-2} \cdot s^{-1} \cdot Pa^{-1}$. This value is too small to account for the large hydrogen permeance difference between membranes A and C, thus it is the membrane thickness that dictates the permeation performance of nanocomposite MFI – alumina membranes.

Please note the defect size scale presented on top of Fig. 2 as obtained from Young-Laplace equation is probably underestimated, since the real porous network is more complex that the simple capillary geometry assumed in the calculation.

4.3. *Influence of pre-treatment on gas separation performance*

Whatever the membrane quality, a desorption step prior to any gas transport performance measurement is compulsory (see Fig. 5). However, all cleaning protocols are not equivalent.

When the desorption step is carried out at lower temperature (200°C) from a membrane previously submitted to air (points β after protocol I and ζ after protocol IV), vacuum is more efficient than air pressure difference. At β, the pure gas permeance is higher, as well as the separation performance. This means that at ζ, some zeolite pores, offering longer diffusion path to desorption, are still blocked by adsorbed species (probably mainly water). The reason of this permeance difference between points β and ζ could then be due to kinetic limitations, as the duration of the treatment is the same for both protocols I an IV. The desorption of blocking species appears faster when the zeolite surface is submitted to vacuum than to a air flow, in spite of the fact that in this case, the gas is forced through the crossing pores.

At 400°C, the application of vacuum seems to favour slightly higher permeances and separation factors (see points γ and δ on Fig. 5). This is a similar effect to that described above at 200°C.

Comparing the two temperatures used in this work (200 and 400°C), one can see that under vacuum no remarkable improvement in separation factor is obtained in the P.T. (see points β and γ), even if some limited gain is observed for the pure permeance. This could be due to the fact that the only effect of a raise of temperature (protocol II) is to open some remaining zeolite membrane pores. Any defect present in the membrane would have been opened by desorption at 200°C during protocol I.

However, when submitted to gas pressure, the influence of temperature is noticeable (see points δ and ζ or η). Even under pressure difference, and with a longer duration (15 vs. 6 h), treatment at 200°C will not achieve complete cleaning of the membranes. This is a well-known temperature effect for desorption. Nevertheless, note that this low-temperature approach is commonly used in literature for membrane cleaning (see Table 1, part b). In those cases, the membrane performances that are reported could be likely underestimated.

Moreover, according to the membrane condition (species present in the pores), the efficiency of the desorption step may differ. For instance, when submitted to open air (i.e. humidity) the membranes are not as well desorbed by protocol IV (air ΔP at 200°C), as when subjected to butane only, see points ε and ζ (Fig. 5). As previously observed [12], water is more strongly adsorbed into highly acidic MFI (as is the case in the present membranes [6]) than n-butane.

To sum up, regardless of membrane quality, the protocols best suited to obtain confident results in characterisations seem to be II or III.

4.4. Importance of membrane quality on membrane pre-treatment effect

Comparing the different membrane P.Ts. without pre-treatment, one can notice that the pure gas permeance is much higher for lower quality membranes (membrane C offers 0.24 $\mu mol \cdot m^{-2} \cdot s^{-1} \cdot Pa^{-1}$, i.e. 33% of the value after application of protocol III at point δ, compared to 0.018 $\mu mol \cdot m^{-2} \cdot s^{-1} \cdot Pa^{-1}$, i.e. 6.6% for membrane A). These measurements were obtained after submitting the membranes to similar atmospheres (room temperature under very low water vapour partial pressure). Under these conditions, as a first approach, water should be condensed only in zeolite pores, and probably not in all of them, as can be inferred on the basis of membrane A permeance (see point α). The difference between the permeance values of membranes A, B and C might be then attributed to defective pores.

Turning from point β into γ through the use of protocol II (vacuum at 400ºC) instead of I (vacuum at 200ºC), it can be observed in Fig. 5 that pure gas permeance remains practically unchanged for the lowest quality membrane (C). However, in the case of membranes A and B, pure gas permeance is promoted. As a matter of fact, in these two membranes, the zeolite pore contribution is higher. Therefore, when desorbing the last remaining adsorbed species after protocol I, the contribution of the newly opened pores is larger for higher quality samples. A similar but lower increase can be observed on the Sf values, arguably for the same reason.

In contrast, when comparing the protocols at 200 and 400°C under gas pressure (points ζ and δ respectively), the trend as a function of membrane quality is reversed from what has been underlined above. In this case, the lower the membrane quality, the less efficient is the 200°C pre-treatment. Membrane C offers 42% lower pure gas permeance than its reference value, while membrane A only 29%. A similar and even more pronounced trend can be seen on Sf values. This could be attributed to the role of transmembrane pressure in protocol IV. In lower quality membranes, defects could be regarded as leaks, through which most of the air permeates, thus by-passing zeolite pores. On the opposite, for high-quality membranes, the air is actually forced through the very zeolite pores, thus desorbing them, and increasing the overall membrane micropore opening efficiency. The introduction of a transmembrane pressure when treating at low temperature broadens the observed difference in membrane quality: low-quality membranes appear worse than they really are.

In the previous section, we mentioned that no major improvement in performance was observed when increasing the temperature from 200 to 400°C under vacuum. However, when looking more closely into the results, a membrane quality effect can be observed. Higher quality membranes benefit from the higher temperature treatment. This could be explained as follows. Let assume that all membranes are opening the same set of remaining pores when submitted to 400°C. Lower quality materials, where a large permeance contribution is due to defects, will not show a major change in flux. Contrarily, in the case of high quality membranes, where the flux is mainly ascribed to zeolite pores, the flux increase will be directly proportional to the number of open zeolite pores. This work clearly showed that membrane reproducibility is not only dependent on the membrane microstructure and composition [1-6, 16, 41-45], but also on the membrane pretreatment. In addition, the experimental conditions in which n-butane/H_2 separations are carried out do also influence the reproducibility: it is not the same working at room temperature that at, for instance, 100-200°C where the steady-state establishes faster.

5. Conclusions

Nanocomposite zeolite – alumina membrane quality appears to be related to the support characteristics. Large defects in the supports tend to cause defect formation in the separative phase, due to incomplete pore plugging. While influencing strongly the gas separation performance of the membranes, these supports defects do not significantly change the single gas permeance of the prepared membrane, which is governed mainly by the thickness of the separative layer.

The other results obtained in this work support the fact that zeolite membrane pre-treatment prior to any gas permeance or separation test is crucial to obtain reliable measurements. The cleaning ability of each desorption protocol not only depends on the plateau temperature and on the pre-treatment gas pressures, but also on membrane quality. In general terms, as could be expected, stronger protocols (vacuum, higher temperature) provide higher performances in permeance and separation, independent of the membrane quality. Interestingly, the introduction of a pressure difference in the desorption step reduces the performance of lower-quality membranes.

Protocols II (vacuum at 400°C) and III (nitrogen at 400°C) appear to be well-suited to later carry out gas permeance and separation measurements. Nevertheless, protocol III offers a good compromise between P.T. results and ease of operation.

Acknowledgements

The Libyan embassy in Paris is greatly acknowledged for A. Alshebani's grant. M. Pera-Titus grant is part of the European Marie-Curie Program (project # 041297).

References

[1] E.E. McLeary, J.C. Jansen, F. Kapteijn, Zeolite based films, membranes and membrane reactors: progress and prospects, Micropor. Mesopor. Mater. 90 (2006) 198.

[2] M. Noack, P. Kölsch, R. Schäfer, P. Toussaint, J. Caro, Molecular sieve membranes for industrial application:

problems, progress, solutions, Chem. Eng. Technol. 25 (2002) 3.

[3] J. Coronas, J. Santamaría, Separations using zeolite membranes, Sep. Purif. Methods 28 (1999) 127.

[4] S. Miachon, I. Kumakiri, P. Ciavarella, L. van Dyk, K. Fiaty, Y. Schuurman, J.-A. Dalmon, Nanocomposite MFI-alumina membranes via pore-plugging synthesis: Specific transport and separation properties, J. Membr. Sci. 298 (2007) 71.

[5] X. Lin, J.L Falconer, R.D. Noble, Parallel pathways for transport in zeolite membranes, Chem. Mater. 10 (1998) 3716.

[6] S. Miachon, E. Landrivon, M. Aouine, Y. Sun, I. Kumakiri, Y. Li, O. Pachtová Prokopová, N. Guilhaume, A. Giroir-Fendler, H. Mozzanega, J.-A. Dalmon, Nanocomposite MFI-alumina membranes via pore-plugging synthesis: preparation and morphological characterisation, J. Membr. Sci. 281 (2006) 228.

[7] P. Ciavarella, H. Moueddeb, S. Miachon, K. Fiaty, J.-A. Dalmon, Experimental study and numerical simulation of hydrogen/isobutane permeation and separation using MFI-zeolite membrane reactor, Catal. Today 56 (2000) 253.

[8] M.A. Snyder, Z. Lai, M. Tsapatsis, D.G. Vlachos, Combining simultaneous reflectance and fluorescence imaging with SEM for conclusive identification of polycrystalline features of MFI membranes, Micropor. Mesopor. Mater. 76 (2004) 29.

[9] G. Bonilla, M. Tsapatsis, D.G. Vlachos, G. Xomeritakis, Fluorescence confocal optical microscopy imaging of the grain boundary structure of zeolite MFI membranes made by secondary (seeded) growth. J. Membr. Sci. 182 (2001) 103.

[10] F. Jareman, J. Hedlund, J. Sterte, Effects of aluminum content on the separation properties of MFI membranes, Sep. Purif. Technol. 32 (2003) 159.

[11] T. Tsuru, Y. Takata, H. Kondo, F. Hirano, T. Yoshioka, M. Asaeda, Characterization of sol-gel derived membranes and zeolite membranes by nanopermporometry. Sep. Purif. Technol. 32 (2004) 23.

[12] O. Pachtová, I. Kumakiri, M. Kocirik, S. Miachon, J.-A. Dalmon, Dynamic desorption of adsorbing species under cross membrane pressure difference: a new defect characterisation approach in zeolite, J. Membr. Sci. 226 (2003) 101.

[13] D. Farrusseng, A. Julbe, C. Guizard, Evaluation of porous ceramic membranes as O_2 distributors for the partial oxidation of alkanes in inert membrane reactors, Sep. Purif. Tech. 25 (2001) 137.

[14] J. Sanchez, C.L. Gîjiu, V. Hynek, O. Muntean, A. Julbe, The application of transient-lag method for the diffusion coefficient estimation on zeolite composite membranes. Sep. Purif. Tech. 25 (2001) 467.

[15] M. Hanebuth, R. Dittmeyer, G.T.P. Mabande, W. Schwieger, On the combination of different transport mechanisms for the simulation of steady-state mass transfer through composite systems using H_2/SF_6 permeation through stainless steel supported silicalite-1 membranes as a model system, Catal. Today. 104 (2005) 352.

[16] J. Hedlund, M. Noack, P. Kolsch, D. Creaser, J. Caro, J. Sterte, ZSM-5 membranes synthesized without organic templates using a seeding technique, J. Membr. Sci. 159 (1999) 263.

[17] M. Yang, B.D. Crittenden, S.P. Perera, H. Moueddeb, J.-A. Dalmon, The hindering effect of adsorbed components on the permeation of a non-adsorbing component through a microporous silicalite membrane: the potential barrier theory, J. Membr. Sci. 156 (1999) 1.

[18] A. Giroir-Fendler, J. Peureux, H. Mozzanega and J.-A. Dalmon, Characterization of zeolite membrane for catalytic membrane reactor application, Stud. Surf. Sci. Catal. 101 (1996) 127.

[19] F. Kapteijn, W.J.W. Bakker, L.J.P. J.M. van de Graaf, G. Zheng, J. Poppe, J.A. Moulijn, Permeation behaviour of a silicalite-1 membrane, Catal. Today 25 (1995) 213.

[20] H.H. Funke, K.R. Frender, K.M. Green, J.L. Wilwerding, B.A. Sweitzer, J.L. Falconer, R.D. Noble, Influence of adsorbed species on the permeation properties of silicalite membranes, J. Membr. Sci. 129 (1997) 77.

[21] T. Matsufuji, N. Nishiyama, K. Ueyama, M. Matsukata, Permeation characteristics of butane isomers through MFI-type zeoltic membranes, Catal. Today 56 (2000) 265.

[22] C.J. Gump, X. Lin, J.L. Falconer, R.D. Noble, Experimental configuration and adsorption effects on the permeation of C4 isomers through ZSM-5 zeolite membranes, J. Membr. Sci. 173 (2000) 35.

[23] V.A. Tuan, J.L. Falconer, R.D. Noble, Isomorphous substitution of Al, Fe, B, and Ge into MFI-zeolite membranes, Micropor. Mesopor. Mater. 41 (2000) 269.

[24] M.P. Bernal, J. Coronas, M. Menéndez, J. Santamaría, Characterization of zeolite membranes by temperature programmed permeation and step desorption, J. Membr. Sci. 195 (2002) 125.

[25] M. Arruebo, J. Coronas, M. Menéndez, J. Santamaría, Separation of hydrocarbons from natural gas using silicate membranes, Sep. Purif. Technol. 25 (2001) 275.

[26] J. M. van de Graaf, E. van der Bijl, A. Stol, K. Kapteijn, J. A. Moulijn, Effect of operating conditions and membrane quality on the separation performance of composite silicalite-1 membranes, Ind. Eng. Chem. Res. 37 (1998) 4071.

[27] T.C. Bowen, H. Kalipcilar, J.L. Falconer, R.D. Noble, Pervaporation of organic/water mixtures through B-ZSM-5 zeolite membranes on monolith supports, J. Membr. Sci. 215 (2003) 235.

[28] J. Coronas, R.D. Noble, J.L. Falconer, Separations of C4 and C6 isomers in ZSM-5 tubular membranes, Ind. Eng. Chem. Res. 37 (1998) 166.

[29] J. Hedlund, F. Jareman, A.-J. Bons, M. Anthonis, A masking technique for high quality MFI membranes, J. Membr. Sci. 222 (2003) 163.

[30] G. Li, E. Kikuchi, M. Matsukata, ZSM-5 zeolite membranes prepared from a clear template-free solution, Micropor. Mesopor. Mater. 60 (2003) 225.

[31] A.J. Burggraaf, Z.A.E.P. Vroon, K. Keizer, H. Verweij, Permeation of single gases in thin zeolite MFI membranes, J. Membr. Sci. 144 (1998) 77.

[32] W.J.W. Bakker, F. Kapteijn, J. Poppe and J. A. Moulijn, Permeation characteristics of a metal-supported silicalite-1 zeolite membrane, J. Membr. Sci. 117 (1996) 57.

[33] S. Gopalakrishnan, T. Yamaguchi, S.-I. Nakao, Permeation properties of templated and template-free ZSM-5 membranes, J. Membr. Sci. 274 (2006) 102.

[34] T.Q. Gardner, J.B. Lee, R.D. Noble, J.L. Falconer, Adsorption and diffusion properties of butanes in ZSM-5 zeolite membranes, Ind. Eng. Chem. Res. 41 (2002) 4094.

[35] Z. Lai, M. Tsapatsis, Gas and organic vapor permeation through b-oriented MFI membranes, Ind. Eng. Chem. Res. 43 (2004) 3000.

[36] M. Lassinantti, F. Jareman, J. Hedlund, D. Creaser, J. Sterte, Preparation and evaluation of thin ZSM-5 membranes synthesized in the absence of organic template molecules, Catal. Today, 67 (2001) 109.

[37] S. Heng, P.P.S. Lau, K.L. Yeung, M. Djafer, J.-C. Schrotter, Low-temperature ozone treatment for organic template removal from zeolite membrane, J. Membr. Sci. 243 (2004) 69.

[38] Y. Yan, M.E. Davis, G.R. Gavalas, Preparation of zeolite ZSM-5 membranes by in-situ crystallization on porous α-Al_2O_3, Ind. Eng. Chem. Res. 34 (1995) 1652.

[39] R. Lai, G.R. Gavalas, ZSM-5 membrane synthesis with organic-free mixtures, Micropor. Mesopor. Mater. 38 (2000) 239.

[40] M. Noack, P. Kölsch, J. Caro, M. Schneider, P. Toussaint, I. Sieber, MFI membranes of different Si/Al ratios for pervaporation and steam permeation, Micropor. Mesopor. Mater. 35-36 (2000) 253.

[41] C. Bai, M.D. Jia, J.L. Falconer, R.D. Noble, Preparation and separation properties of silicalite composite membranes, J. Membr. Sci. 105 (1995) 79.

[42] V.A. Tuan, J.L. Falconer, R.D. Noble, Alkali-free ZSM-5 membranes: preparation conditions and separation performance, Ind. Eng. Chem. Res. 38 (1999) 3635.

[43] W.C. Wong, L.T.Y., Au, C. Tellez, K.L. Yeung, Effects of synthesis parameters on the zeolite membrane growth, J. Membr. Sci. 191 (2001) 143.

[44] L.T.Y. Au, W.Y. Mui, P.S. Lau, C. Tellez, K.L. Yeung, Engineering the shape of zeolite crystal grain in MFI membrane and their effects on the gas permeation properties, Microporous Mesoporous Mater. 47 (2001) 203.

[45] L.T.Y. Au, K.L. Yeung, An investigation of the relationship between microstructure and permeation properties of ZSM-5 membranes, J. Membr. Sci. 194 (2001) 33.